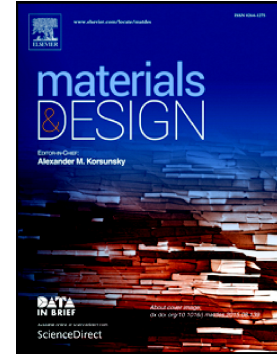# Accepted Manuscript

Pin-on-disc study of brake friction materials with ball-milled nanostructured components

Cinzia Menapace, Mara Leonardi, Guido Perricone, Mauro Bortolotti, Giovanni Straffelini, Stefano Gialanella

Please cite this article as: Cinzia Menapace, Mara Leonardi, Guido Perricone, Mauro Bortolotti, Giovanni Straffelini, Stefano Gialanella , Pin-on-disc study of brake friction materials with ball-milled nanostructured components. The address for the corresponding author was captured as affiliation for all authors. Please check if appropriate. Jmade(2016), doi: 10.1016/j.matdes.2016.11.065

PIN-ON-DISC STUDY OF BRAKE FRICTION MATERIALS WITH BALL-MILLED NANOSTRUCTURED COMPONENTS.

Cinzia Menapace*[1], Mara Leonardi[1], Guido Perricone[2], Mauro Bortolotti[1], Giovanni Straffelini[1], Stefano Gialanella[1]

[1]Department of Industrial Engineering, University of Trento, Trento, Italy.

[2]Brembo S.p.A, Bergamo, Italy

*: corresponding Author

ABSTRACT

Copper is an ingredient of the automotive disc brake pads with important functional role. On the other hand, copper is regarded as one of the most hazardous component of the particulate matter released by the brake linings. Legislation in several countries is progressively reducing the tolerated amount of copper in friction materials. In this work, a possible approach to the reduction of copper in brake friction materials is presented. Starting from a commercial, state-of-the art, non-asbestos organic friction material, different formulations have been prepared, changing the microstructure of some of the ingredients, namely copper and zirconia using high energy ball-milling. The wear behavior of the newly developed materials has been tested and validated using pin-on-disc wear tests. One interesting aspect observed is that the wearing out of copper fibers produces fine copper particles entering the friction layer, thus contributing to its compaction. This observation implies that copper powder is not strictly required as a component in the starting friction material to achieve anyway a satisfactory tribological behavior associated with a stable friction layer. Furthermore, the addition of milled components provided interesting indications to be explored further in view of the replacement of copper in brake friction materials.

KEYWORDS –

Disc brake; friction material; friction layer; high energy ball-milling; copper reduction.

1. INTRODUCTION

Wear phenomena occurring at the contact region between disc and pad in brake systems result in the consumption of the involved materials with a consequent release of particulate matter (PM) in the environment [1]. The presence of fine and ultra-fine fractions, with aerodynamic diameter below 10-2.5 μm (PM_{10} and $PM_{2.5}$) and 0.1μm ($PM_{0.1}$) respectively, has been reported and this is posing increasing concern for the public health and environmental pollution [2]. According to a UN survey [3], brakes contribute to the total non-exhaust vehicular emissions for a weight percentage ranging from 16% up to 55%. This situation is the obvious consequence of the lack, at least until recent, of important research

efforts in this field, similar to those that have lead to the major reduction of emissions from internal combustion engines of road vehicles.

The wear behavior of brake linings results from the interplay of operating conditions, including the braking style of the drivers, and brake materials [4-7]. Important requirements for brake materials are: excellent stability under any operating condition and low PM emission rate. Wherereas the most common and widespread car brake discs are made of plain gray cast iron, friction materials for pads, particularly the so-called organic friction materials, are complex mixtures of different ingredients, usually grouped into the following categories: reinforcements, metals, friction modifiers (lubricants and abrasives), fillers and binders [8-11].

The relative sliding of the pads and disc determines the formation of the so-called friction layer, made of the wear debris blocked by the reinforcements (primary plateaus) to form compacted continuous patches (secondary plateaus) [12]. This sequence results from the prefential wearing out of the softer ingredients of the pads, mainly by abrasion, and by the tribo-oxidation of the disc, producing iron oxide particles. Correspondingly, the reinforcements of the friction material, mainly metallic fibres and hard particles, start protruding from the pad surface and thus contribute to the compaction of wear debris to form the mentioned secondary plateaus. Of course, the shear stresses associated with the sliding against the disc surface tend to detach the friction layer from the surface of the pads and of the disc too, and a sort of dynamic equilibium between these two tendencies is accompanying the whole life span of the disc-pad system [13].

Usually, copper is present in brake pads of road vehicles both as powder and fibres, with concentrations in the 5-20% range. Much lower values are under discussion for standards and legislation, implemented already in some of the US member states [14,15]. This trend will unavoidably lead to the elimination of copper from brake pads within the next ten years or so. Indeed, brake pads are regarded as the main source of copper released in urban areas [16]. Considering the acknowledged toxicity of copper, with an established incidence on environmental conditions and human health [17-19], its elimination from brake friction materials has become a major issue. As concerns the environmental aspects, it has been reported that 35-50% of the wear debris emitted by the vehicle brake linings are airborne [20-21]. The high fraction having average particle size in the submicrometric range (ultra-fine particulate matter, UFP) and the relevant copper content, renders this debris particularly dangerous, since it can directly access the deeper pulmonary regions and, from there, blood circulation [22]. Like other metals present in PM, air suspended copper may trigger the formation of reactive oxygen species (ROS) in biological tissues with consequent oxidative stresses [23-25]. Larger non-airborne wear fragments have detrimental and toxic effects on aquatic species, whose environment may be contaminated by rain-washed copper [26].

On the other hand, copper has a fundamental role in brake pad friction materials. Copper fibers act as reinforcements and contribute to the formation of the primary plateaus. Copper particles, possibly coming from the wearing out also of the fibers, enter the friction layer, that, thanks to copper, becomes denser and better adherent to the mating surfaces of the pad and disc [27-29]. Consequently, the tribological contact becomes more stable, with important beneficial effects on the braking action and vehicle comfort, thanks to the elimination of the disturbing "squeaking" effects [30].

2

The scope of the present study is twofold. First, producing novel compositions of friction materials featuring reduced copper concentration, starting from a commercial product. For the validation of the wear performances, cylindrical pins manufactured out of the new materials are wear tested by dry sliding PoD (pin-on-disc) against a cast iron disc. For this approach, suggested by similar literature studies [19], mild wear conditions, interesting for these systems [31-34], have been adopted. The relevant wear results are meant to provide indications to design completely copper-free formulations for brake friction materials, still featuring excellent tribological properties in association with a low emission rate of airborne particulate matter, with particular regard for the ultra-fine fraction.

In view of the mentioned role of copper in the formation of a compact and stable friction layer, the leading idea of the present work is to introduce this element in the friction material with a nanostructured morphology of the grains, that turns out to be the right microstructure of copper particles to form an optimal friction layer [27, 35]. Copper powder with this refined microstructure can directly enter the friction layer since the early stages of its formation, without the need to be produced *in situ* during the running-in stage of the wear tests. It is also evident that the availability of nanostructured copper in the friction material is a prerequisite to cut down its total concentration to the value stricly needed for the formation of the friction layer itself. It is worth saying that in commercial brake pads copper is there also to enhance the otherwise low thermal conductivity, so that the frictional heat produced by the braking action is dissipated effectively. For this purpose, copper, and other metal alloys, like steel and brass, are introduced into the friction material as fibres. However, the usage of metallic fibres for increasing the thermal conductivity in brake pads is still rather controversial. Indeed, the thermal conductivity of the friction materials typically ranges between 0.5 and 3 W/mK. Therefore, it is considerably lower than that of the cast iron, the disc material. Furthermore, the inclusion of metal led to an enhancement in friction performance of the composites but at the cost of wear resistance [36,37]. In the present study the focus was on the powder components of the friction material only. Therefore, the fraction of fibres, both of copper and steel, present in the master mixture was left unaltered.

For the refinement of the grain size of the copper powder, high-energy ball-milling has been chosen, since this processing technique has been found particularly effective for producing fine grained metallic materials [38, 39], it is comparatively cheap, can be easily and profitably scaled up from lab to industrial size productions, that are actually less critical, since a larger amount of processed powder usually helps overcoming the contamination problems that can be faced when dealing with small batches.

2. EXPERIMENTAL PROCEDURE

2.1 THE MATERIALS

As reference material for this work, a commercial NAO (non-asbestos organic) pad material was used. It is referred to in the following as Original Mix, *OM*. In Table 1, the main components and relevant concentrations in the *OM* are summarized. They can be classified as: frictional additives (zirconia, potassium titanate, graphite, tin sulfide, aluminium oxide), fillers (vermiculite, barite, calcium

carbonate), reinforcing fibers (steel and copper fibers) and a binder (phenolic resin). Actually, copper is present in the *OM* not only in the form of fibers but also as micrometric powder (see below specifications and Fig. 1b). This is the component that has been varied to different extents to produce friction materials with novel compositions. In particular, three powder mixtures have been prepared:

- one with unaltered concentration of the copper powder, although this has been introduced in the mix after high-energy ball-milling, following the procedure described in section 2.2. Material codename: *100 CP*.
- The second material has been prepared following the same protocol as the previous one, but with just 50% of the copper powder content. Material codename: *50 CP*.
- The third material contains no copper powder at all. Material codename: *0 CP*.

It is worth reminding that in all materials, *0 CP* included, copper fibers were anyway present to the same extent as in *OM*. They will play a decisive role in determining the tribological response of the friction materials.

Compounds	Wt%	Compounds	Wt%
Zirconia (ZrO_2)	22.5	Alumina (Al_2O_3)	3.0
Mg oxide (MgO)	6.9	Calcite ($CaCO_3$)	2.5
Iron (Fe)	8.0	Tin Sulfide (SnS)	2.5
Copper (Cu)	10.0	Zinc (Zn)	2.0
Vermiculite	6.0	Bismuth (Bi)	0.6
Barite ($BaSO_4$)	5.0	Iron Sulfide (FeS)	0.5
Potassium Titanate ($K_2O_6TiO_2$)	5.0	Rest (phenolic resin, graphite)	

Table 1. Main compounds, and concentration, in the brake pad material (Original Mix - *OM*).

2.2 HIGH-ENERGY BALL-MILLING

The copper powder fraction was added to *100 CP* and *50 CP* materials after a preliminary ball-milling, intended to reduce its average grain size. Ball-milling was carried out introducing into the vial (made of M2 tool steel) the metallic powder, preliminarily mixed with zirconia and graphite, in the right *OM* concentration. This was made in order to prevent too diffuse cold-welding of copper during ball-milling exploiting the role of process control agent of zirconia and, particularly, graphite powders. Moreover, mixing together copper and zirconia, would have produced a fine dispersion of the two components, with potentially beneficial effects on the formation of the friction layer during tribological pin-on-disc testing. As reported [32], the friction layer obtained from wear tests using pins made of *OM* material dry sliding against a cast iron disc, features, as majority phases, iron oxides from the disc and zirconia from the pin, both held together and compacted, to form secondary plateaus, by copper wear debris.

Zirconia (mean particle size of 10 μm), copper (50 μm long dendrites, see Fig. 1), and graphite powders were milled at room temperature, under rotary pump vacuum, using a planetary ball-mill (Fritsch Pulverisette 6). The speed of rotation was 400 rpm and the process time was 10 h. The mill was set up in reverse mode, which allows to reverse the direction of rotation at each cycle (1 hour) in

4

order to improve the homogenization level of the powder. The ball-to-powder weight ratio was 10:1 (1000 g of 20 mm chrome steel balls with 100 g of powder). Two powder mixtures with different Cu/ZrO_2 ratio, in order to preserve the right composition of the *OM* material, were ball-milled :

  (A) ZrO_2 and Cu powder with a 15:1 ratio, used for the *100 CP* material;

  (B) ZrO_2 and Cu powder with a 30:1 ratio, used for the *50 CP* material.

Graphite (1 wt.%) added to both mixtures A and B, as expected, turns out to be very effective in reducing powder welding during milling, leading to a comparatively high yield in the process, close to 100% recovery of the powder from the vial.
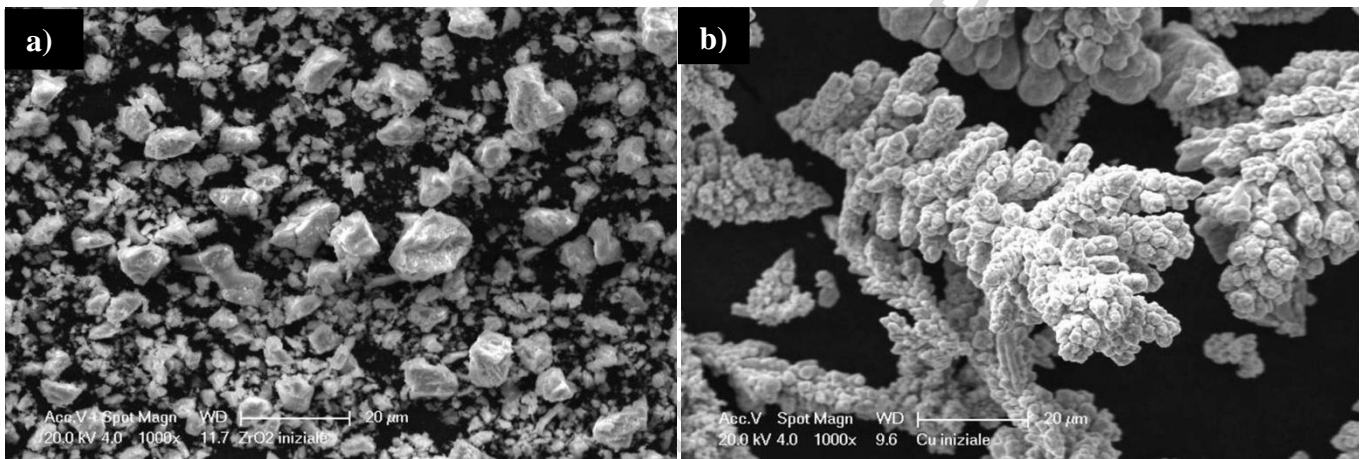

Fig.1: Microstructure of two starting milling materials, a) zirconia and b) copper powder.

2.3 POWDER MIXING AND PIN PRODUCTION

In Table 2 the codenames and the main characteristics of the three powder mixtures produced are summarized. Ingredients were mixed in the turbula shaker-mixer to ensure a complete homogenization. For all samples a quantity of 100 g was shaker-mixed for 20 min. In 100 CP and 50 CP, milled powder mixtures A and B (described in 2.2) were added; while in 0 CP, ZrO_2 and graphite were added in the as-supplied condition.

Table 2. Designation of samples and relative content (wt%) of raw materials.

Ingredients (wt%)/Designation	OM	0 CP	100 CP	50 CP
Original Mix	100.0	-	-	-
New parent mix[a]	-	75.8	75.8	75.8
Zirconia	-	24.0	22.5	23.2
Copper powder	-	0.0	1.5	0.8
Graphite	-	0.2	0.2	0.2

[a] Original Mix without copper powder and zirconia.

5

The mixtures were used to produce cylindrical pins, for the wear testing, using a cylindrical mold placed in a hot-pressing apparatus typically used for metallographic sample preparation. Using 1 g of powder mix, pins of 6.0 mm in diameter and 9.0 mm in height were produced. The process temperature during hot-pressing reaches about 150 °C. The pins remain under compression for 15 min, and then are post-cured in an industrial oven at 200 °C for 10 h. After production, the pins are surface finished with a SiC 800 grit abrasive paper in order to remove scraps from the processing. Samples produced in this way were compared with pins cut from industrial brake pads made with the same material [32] and both microstructure and density were seen to be comparable.

As counterface material in the PoD tests, a pearlitic grey cast iron disc with a hardness HV10 of 235 was used.

2.4 PIN-ON-DISC CONFIGURATION

For reliable PoD tests, carried out on a Eyre/Biceri pin-on-disc tribometer, it is essential that the surface of the pin is flat, so to have a conformal contact with the disc. It has been obtained inserting the pin in a cilindrical die with strict tolerance (in order to avoid any deflection into the die cavity) and grinding it on a SiC paper before the wear test.The wear of the pin is evaluated by measuring its weight before and after each test. An analytical balance with a precision of 10^{-4} g was used. Data were converted into wear volumes using the densities measured for the friction materials which are 2.90 ± 0.04 g/cm^3 for *OM* composition, 2.89 ± 0.03 g/cm^3 for *0 CP*, 2.90 ± 0.05 g/cm^3 for *100 CP*, 2.89 ± 0.06 g/cm^3 for *50 CP*. The density of each pin was measured diving its weight by its volume, while wear volumes (V expressed in m^3) are obtained simply dividing the weight loss (expressed in grams) by the density of the pin (g/cm^3 * 10^6). Wear tests were carried out at a sliding velocity v=1.57 m/s and nominal contact pressure p_0=1 MPa.

Two tests were conducted for each sample at room temperature. The duration of the test was 50 minutes and at the beginning of each test, a 10 min run-in period was allowed to attain a stable contact between pin and disc. Longer tests (5h) were also conducted for each sample in order to collect a larger amount of wear fragments.

During PoD tests, the friction coefficient was continuously recorded as well as the contact temperature. For this purpose, two chromel-alumel type thermocouples were placed in two holes drilled in the pin holder in contact with the pin itself. To estimate the average contact temperature, the frictional heat flow was considered to be one-dimensional and the temperature was then assumed to decrease linearly from the contact surface (pin-disc) going upward.

2.5 MATERIALS AND WEAR PRODUCTS CHARACTERIZATION

The crystalline phases and their composition in the ball-milled powders (zirconia and copper) were identified using X-ray diffraction (XRD) measurements carried out with an Italstructures IPD3000 instrument equipped with a Cu anode source (fine focus) operating at 40 kV and 30 mA. A multilayer monochromator was used to suppress k-beta lines from the incident radiation, with a dual fixed-slit setup (100 microns) to reproduce a quasi-parallel beam. Diffraction spectra were acquired in reflection geometry (fixed omega=5°) over a 5-125 degree range by means of an Inel CPS120 curved position sensitive detector. The instrument was preliminarily calibrated with a NIST 660b LaB$_6$ standard reference material. XRD data were modeled by means of a full-pattern approach based on the Rietveld

6

method as implemented in the Maud software. The sample model was setup as a multi-phase mixture, accounting for monoclinic and tetragonal ZrO_2 as well as metallic Cu. Modeling parameters included, besides the crystal phases volume fractions and the scale factors, the average crystallite sizes for all the phases.For a comparative evaluation of the different materials, the specific wear coefficient (K_a), was used, calculated as [40]:

$$K_a = V / F_n \, s$$

where V [m^3] is the measured wear volume, F_n [N] is the applied load and s [m] is the sliding distance. The surface morphology of the worn pads was observed with a scanning electron microscope (SEM). SEM cross-sectional observations were also used to investigate the microstructure of the friction layer building up on the pin surface during the PoD tests. With energy dispersive X-ray spectroscopy (EDXS) the composition of the primary and secondary plateaus was measured and the elemental surface distribution was analyzed with EDXS-mapping.

3. RESULTS AND DISCUSSION

3.1 BALL-MILLED POWDER MIXTURE CHARACTERIZATION

Fig. 2 shows the XRD pattern of the copper-zirconia-graphite "A" powder mixture before and after ball-milling. In Table 3 the average crystallite size for the majority component phases are listed for the two ball-milling mixes: A and B.
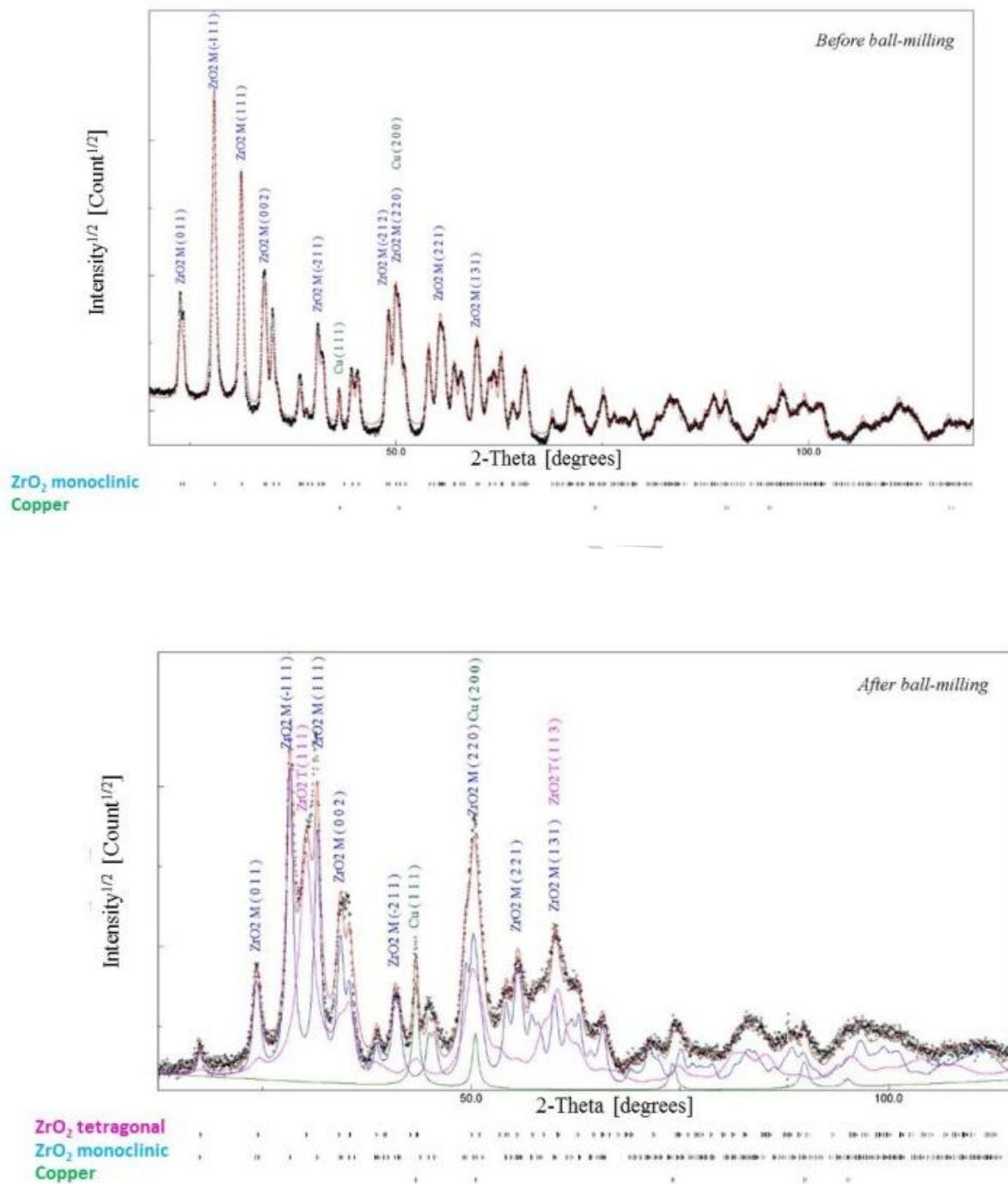
Fig.2: XRD of the "A" mixture before and after ball-milling. Dot: experimental points; continuous line: Rietveld simulated pattern.

Graphite does not appear among the analyzed phases, since its concentration is too low to provide sufficiently intense diffraction signals. High-energy ball-milling induces the partial transformation of the original monoclinic zirconia phase, stable at room temperature, into the tetragonal high temperature polymorph. This stress induced martensitic transformation has been reported already in previous studies on high-energy ball-milling of zirconia powders [41,42]. Another, expected result of ball-milling is the reduction of the average crystallite size, <D>, of both metallic and ceramic phases, due to the extremely high mechanical strain involved with high-energy ball-milling. The values of the average cristallite size of all phases are in a typical range for nanostructured materials.

	<D> (nm)			
	Before milling		After milling	
	A	B	A	B
Cu powder	>700	>700	15.3	15.3
ZrO_2 monoclinic	348	348	14.0	12.8
ZrO_2 tetragonal	-	-	6.0	6.1

Table 3. Average crystallite size of Cu and ZrO_2 phases in the powder mixtures A and B, before and after ball-milling (speed of rotation=400 rpm, miling time=10h, ball-to-powder weight ratio=10:1).

The morphology of the powders after ball-milling is shown by the SEM micrograph in Fig. 3, referring to both A and B mix. The presence of clusters of grains is observed in the two samples, although in the former (A) these clusters appear to be more numerous and bigger than in B material. In the optical micrograph in Fig. 4, the metallographic section of the B powder is displayed. Comparatively coarse clusters of zirconia feature a fine dispersion of copper particles (see arrowed region in Fig. 4). This confirms that the ball-milling was successful in obtaining a significant reduction of the copper grain size, coherently with the reduction in the average crystallite size proved by the XRD data (Tab. 3). These copper grains are finely dispersed into the ceramic zirconia powder. However, the intermixing of the two phases (copper and zirconia) has also produced the formation of the powder clusters displayed in Fig. 3, that, as it will be shown in the following, will not have a completely positive effect on the tribological behavior of the relevant friction materials. From the results of a preliminary survey study conducted to choose the suitable milling conditions, it seems that an effective approach to reduce the agglomeration is by changing the concentration of graphite in the starting mix. This element would in fact reduce the tendency to form too coarse grains of powder.

Another aspect concerning the milling step is the contamination from the milling media. An estimated iron contamination from the vial and balls equal to 2 wt% and 4 wt% was measured for the A and B material respectively. Altough it is important to control this parameter too in view of the full qualification of the friction materials, the effect of iron contamination seems to be really negligible.
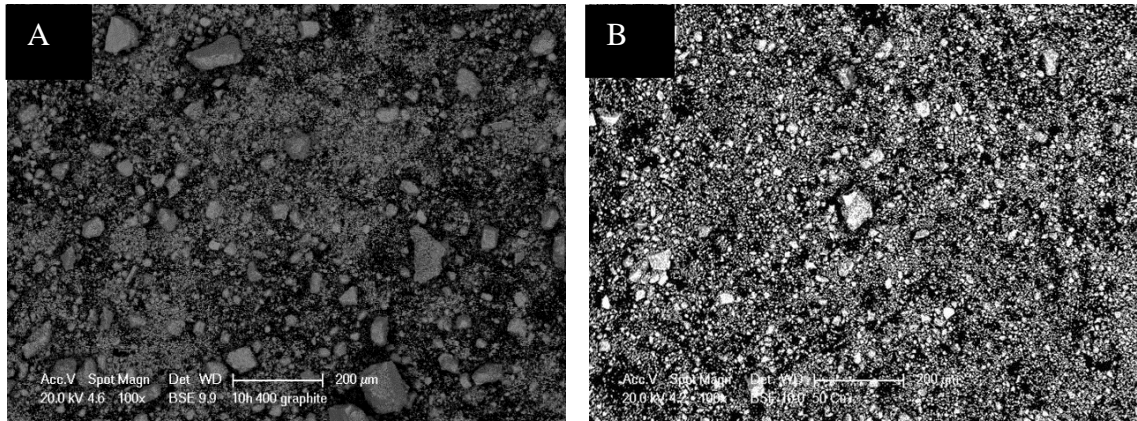
Fig.3: SEM micrographs showing the microstructure of the powder mixes A and B after high Energy ball-milling.
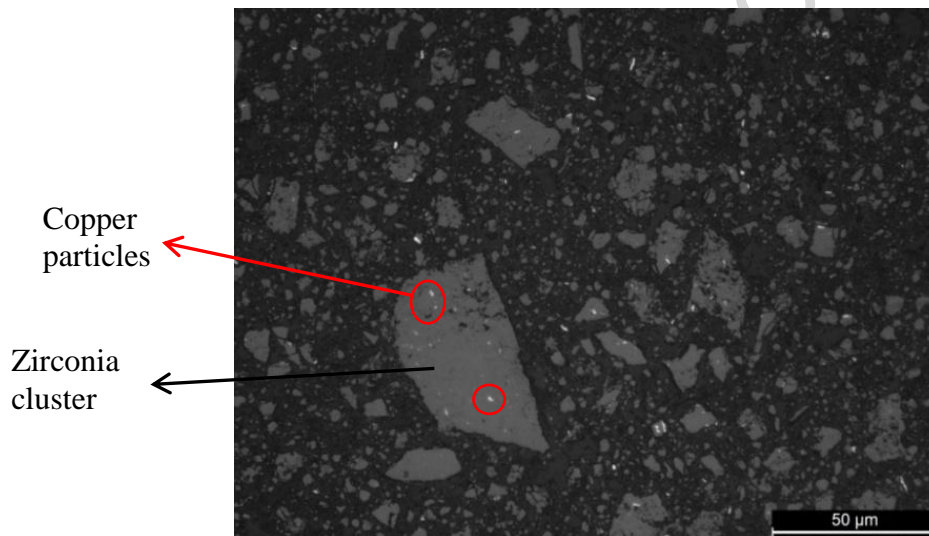

Fig.4: Optical microscopy observation of the metallographic section of the "B" material after milling, Copper particles are visible within the zirconia clusters.

3.2 PIN CHARACTERIZATION

In Fig. 5, the EDXS Cu X-ray maps are shown for a comparison between the materials *0 CP* and *OM*, as concerns the difference in copper content and distribution. Copper fibres are present in both materials, whereas copper powder is only present in the OM material. The other component of the original friction material that has been considered in this investigation is zirconia. The X-ray maps of zirconium were acquired on the same areas as the maps of Cu in Fig.5: the corresponding SEM micrographs are shown in the left column of Fig.6. ,The results (Fig.6, right column) indicate that this element, present as zirconium oxide, is uniformly distributed within the *OM* friction material and in its derivative *0 CP*, without any copper powder, but just fibres. Zirconia clusters, already commented upon in the previous section on ball-milling (see Fig. 3 and 4), are now visible also in the pins made of the *50 CP* and *100 CP* materials.
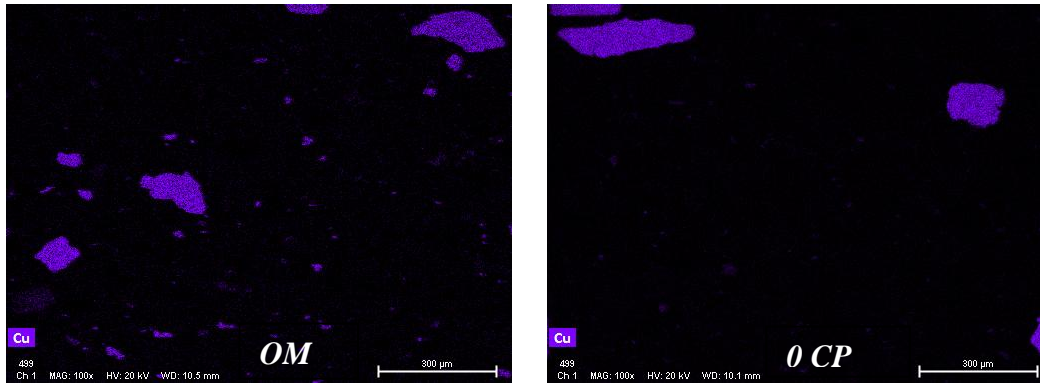
10

Fig.5: Cu X-ray maps for the *OM* and *0 CP* materials, displaying a substantial equivalence, as concerns the presence and distribution of copper fibres. As to powder component, copper is present in the *OM* material only. The maps were collected on the micrographs presented in Fig. 6.

At higher magnification, these regions shows they have a different microstructure in the *100 CP* and *50 CP* materials (Fig. 7). In particular, the lower concentration of copper results in less compact zirconia clusters, as was to be expected. The higher Fe contamination from the milling media in the *50 CP* material, as compared to the *100 CP*, is compatible with the difference in the contrast of the relevant Fe X-ray maps.
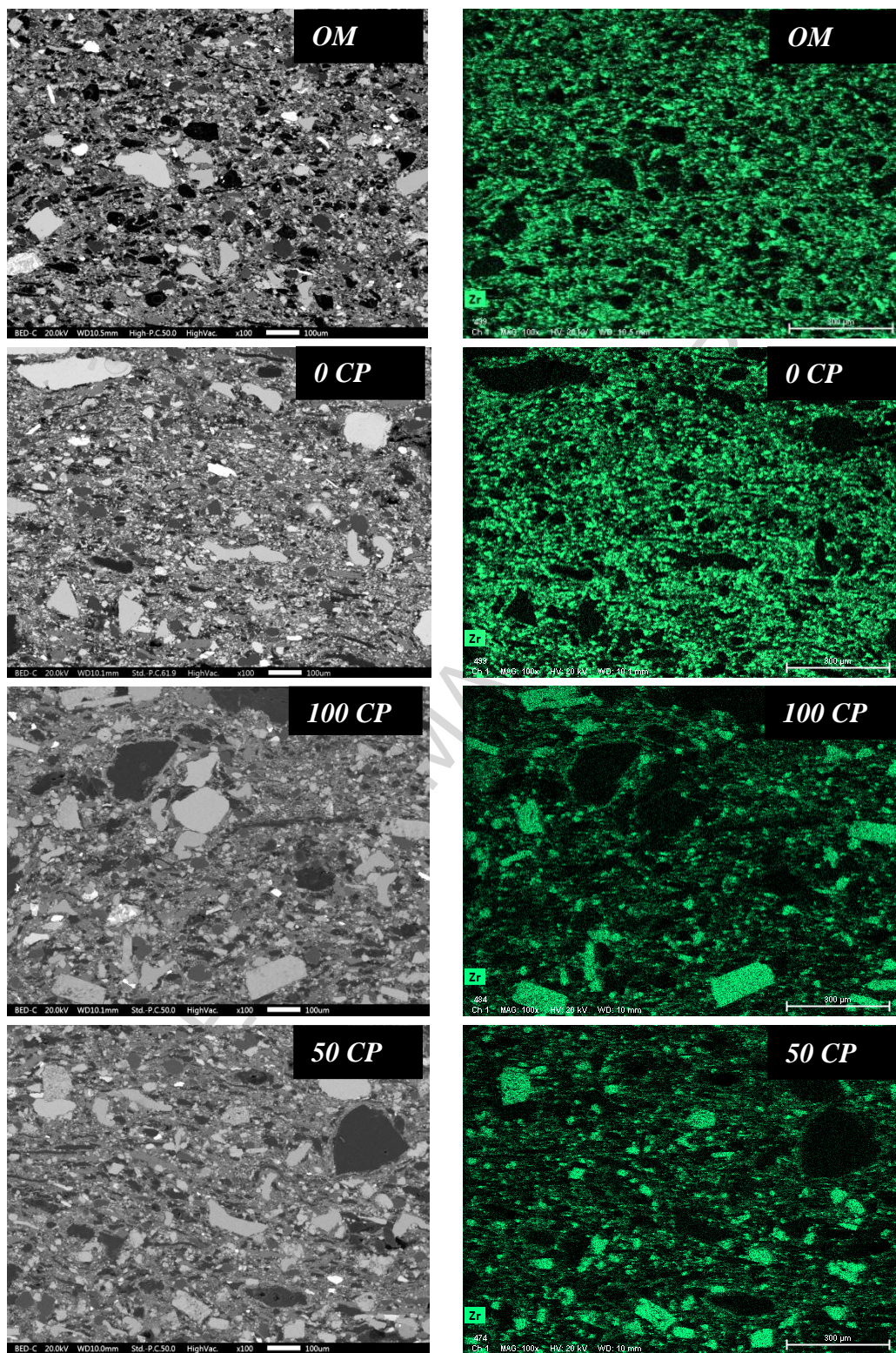
11

Fig.6: SEM micrographs of the pins cross-sections of the materials: *OM, 0 CP, 100 CP, 50 CP*. The relevant X-ray maps for zirconium, show the distribution of this element, present as zirconia in the friction materials.
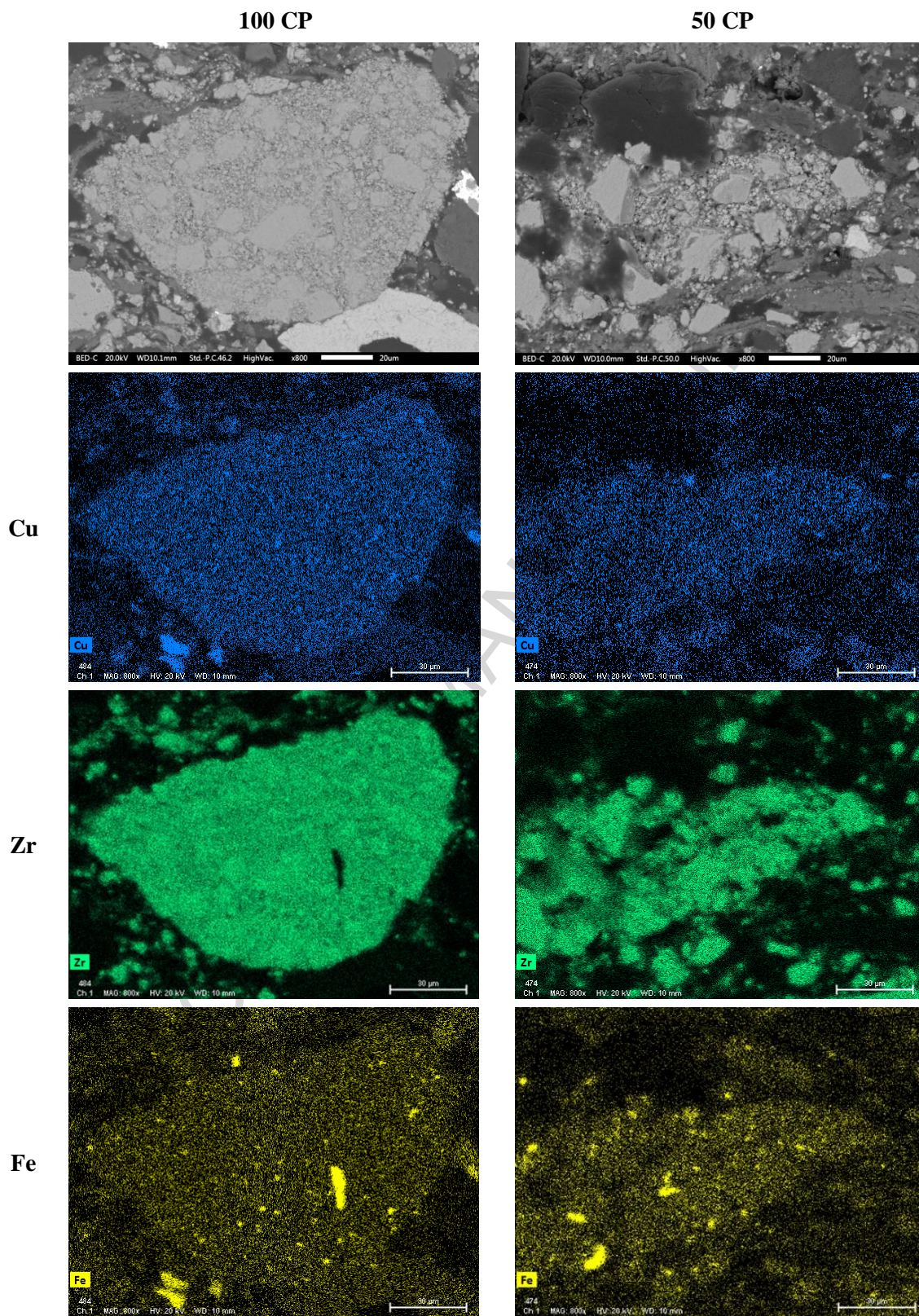
12

Fig.7: SEM micrographs and relevant X-ray maps for Cu, Fe and Zr of the pins made of the *100 CP* e *50 CP*. Clusters of zirconium oxides are visible, in agreement with the observations on the as-milled powders (see Fig. 3). Patches of non-homogenized, possibly un-milled, material are also visible in the friction material.

13

3.3 FRICTION AND WEAR

Fig.8 shows the evolution of the coefficient of friction, μ, for the different materials as recorded during the PoD tests conducted for 50 min. The *0 CP* specimen has a substantially constant trend with time, very similar to what observed for the *OM* sample. In particular, after 600 s run-in approx., the pin-disc contact gets stabilized and the friction coefficient remains at a steady state value until the end of the test. For the *100 CP* and *50 CP* materials, an initially increasing, with time, friction coefficient is observed, that achieves a constant value only after 800 s. This value is retained for the rest of the test. It seems that a longer run-in is necessary for the 100 CP and 50 CP than for the other two materials. This different behavior is ascribable to the different microstructure induced in the two sets of sample by the ball-milling of the copper-zirconia-graphite mix. In Table 4 the average values of the friction coefficients recorded during PoD test carried out with the four friction materials for short (50 min) and long (5h) times are shown. These values are all compliant with those obtained in PoD studies, involving standard brake friction materials [9, 32, 43].
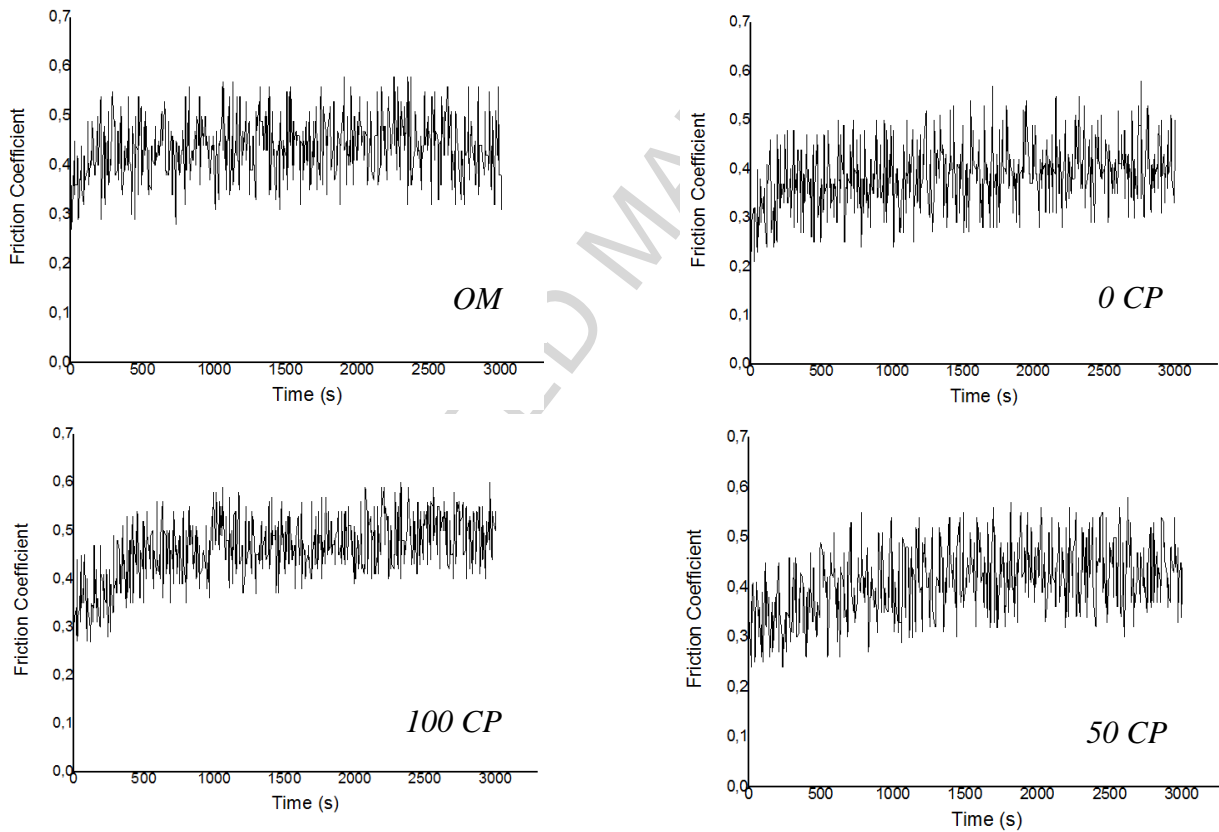

Fig.8: Evolution of the friction coefficient for the four materials considered in this study recorded during the PoD tests carried out for 50 min.

	μ		K_a (m^2/N)	
	50 min	**5 h**	**50 min**	**5 h**
OM	0.42±0.06	0.46±0.05	$5.26*10^{-15}\pm1.39*10^{-15}$	$3.34*10^{-15}\pm1.16*10^{-15}$
0 CP	0.40±0.07	0.45±0.05	$3.70*10^{-15}\pm1.29*10^{-16}$	$2.56*10^{-15}\pm2.34*10^{-16}$
100 CP	0.46±0.07	0.45±0.06	$2.32*10^{-14}\pm8.67*10^{-15}$	$3.03*10^{-15}\pm6.67*10^{-16}$
50 CP	0.43±0.07	0.54±0.07	$1.27*10^{-14}\pm9.81*10^{-16}$	$1.62*10^{-14}\pm1.01*10^{-15}$

Table 4. Coefficient of friction and specific wear coefficient for the PoD test carried out for short (50 min) and long (5h) times.

The specific wear coefficient (K_a) can be taken as an indicator of how severe wear is. In Table 4, the values for the coefficient of friction and specific wear coeffcient for the four friction materials are listed.They refer to short (50 min) and long (5h) term PoD tests. For the short term tests, the *100 CP* and *50 CP* materials exhibit a K_a of $2.32*10^{-14}$ m^2/N and $1.27*10^{-14}$ m^2/N respectively. Under the same test conditions, the *OM* and *0 CP* materials both display a specific wear coefficient one order of magnitude lower, in the 10^{-15} m^2/N range, as an indication of a better wear resistance. This is also confirmed by Fig. 9. The graph in this figure shows the evolution of the specific wear coefficient and it is drawn using the data in Table 4. The *OM, 0 CP* and *100 CP* materials all display a decreasing trend of the wear coefficient with time. In particular, the *100 CP* reaches a comparable value of wear coefficient ($3.03*10^{-15}$ m^2/N) as the *OM* and *0 CP* materials in the long term PoD tests. The *50 CP* is the only one of the four materials displaying an increasing trend, i.e., its wear resistance turns out to be lower for longer testing times. Moreover, it is important to highlight that the values of both μ and Ka of *OM* are by all means comparable to the values obtained with *OM* pins cut out from real brake pads and tested in the same conditions [32].

The wear rate of the couterface discs has been also investigated. With a stylus profilometer, the wear tracks left on the disc surface by the sliding pin have been measured to evaluate the volume of wear and, thereby, the specific wear coefficient (see Table 5) for all discs, but the one tested against the *0 CP* material. In this case, no detectable wear of the disc has been recorded. It can be noticed that in all cases a mild wear of the discs was observed, coherently with the wear coefficient of the friction materials (see Table 4).
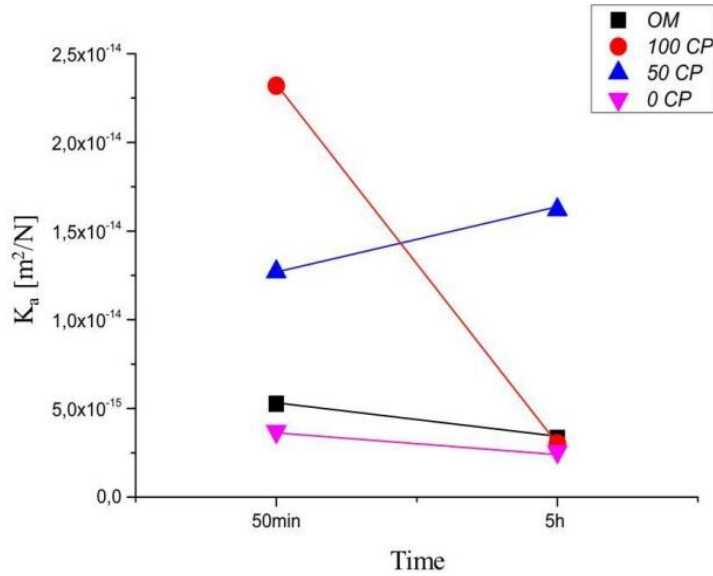
Fig.9: Specific wear coefficient obtained with the four materials analyzed in the present study as a function of the duration of the PoD tests.

	K_a (m^2/N)
OM	$9.14*10^{-15}$
100 CP	$1.42*10^{-14}$
50 CP	$9.79*10^{-15}$
0 CP	Not Detectable

Table 5. Specific wear coefficient of the cast iron discs – Data referring to 50 min PoD tests.

3.4 ANALYSIS OF WEAR SURFACE

To complete the picture provided by the tribological parameters, i.e., μ and K_a, in order to gain a better insight into the wear mechanisms, the wear tracks on the pin surface were investigated by SEM observations and EDXS analyses. In particular, the main components of the friction layer and relevant composition were measured.

Fig. 10 shows the top view of the friction layers that formed on the surface of the four friction materials. According to a consolidated pattern [12], the two main component parts of the friction layer are: the primaty plateaus, made of the metallic fibres, and the secondary plateaus. These latter are produced by the compaction of the wear debris trapped in between the two mating surfaces. The formation of the secondary plateaus is in fact favored by the presence of the primary plateaus, that

16

block the debris and promote their piling up. The *OM* and *0 CP* samples display a good compaction of the debris to form the secondary plateaus at the interface with the metallic fibres. The overall stability of the friction layer is compatible with the low measured wear coefficients (Table 4), that in fact are in the 10^{-15} m^2/N range, the lowest recorded in the present investigation, irrespective of the duration of the PoD tests.

After the short term PoD tests, the friction layers observed on the *50 CP* and *100 CP* materials display an important difference with respect to the other two materials. The primary plateaus are partially covered by wear debris, that form a sort of extended secondary plateaus, although they are not so well compacted and, thereby, protective like the secondary plateaus forming on the *0 CP* and, particularly, the *OM* materials. The different character of the secondary plateaus on the *OM* and *0 CP* materials as compared to the secondary plateaus forming on the *50 CP* and *100 CP* pins can be clearly inferred from the cross sectional X-Ray maps for zirconium and iron in Fig.11. In the *OM* and *0 CP* samples, the secondary plateaus would feature the coexistence of finely dispersed particles of zirconium and iron oxide to form well compacted layers. The zirconia particles come directly from the friction material, where they are homogeneously distributed (see X-Ray maps in Fig. 6). As concerns iron oxide particles, they come from the tribo-oxidation of the cast iron disc. Iron is the majority element in the secondary plateaus that form on the *50 CP* and *100 CP*, as shown by the X-Ray maps in Fig. 11 and by the EDXS data of the secondary plateaus forming on the four friction materials plotted in Fig. 12. The higher concentration of iron in the secondary plateaus forming on the *50 CP* and *100 CP* materials, in association with the higher K_a values of the specific wear cofficients, confirm an important material transfer from the disc onto the pin. The particularly high concentration of iron detected in the secondary plateaus forming on the *50 CP* material, suggests that in addition to the tribo-oxidation of the cast iron disc, other mechanisms, like abrasion of the disc surface, are now active. This situation is determined by the impossibility of forming a truly protective friction layer by the *50 CP* and *100 CP* materials. The reason for this is attibutable to the inhomogenoeus distribution in the starting friction materials of two essential components of the secondary plateaus: zirconia and copper, for the clustering induced by ball-milling (see Zr map in Fig. 6). The spreading of the wear fragments over the metallic, copper and steel fibres has another important consequence: it prevents the abrasion of these fibres and consequent release of metallic fragments. These fragments, particularly copper particles, have an essential role in the formation of the secondary plateaus. Interestingly, in the *0 CP* sample, notwithstanding the complete absence of copper powder in the formulation of the friction material, still the contribution of copper coming from the abrasion of the fibres is sufficient to reach a suitable concentration (see Fig. 12) for a successful formation of stable secondary plateaus.

Actually, for longer PoD test time (5h) the situation changes as concerns the *100 CP* material, that at this stage displays a friction layer absolutely similar to the friction layer observed on the best wear performing materials, *OM* and *0 CP*, as shown by the SEM micrographs in Fig. 13. It is also evident that unsatisfactory secondary plateaus are still forming on the *50 CP* instead, having the same structure as those observed after the short term PoD tests (Fig.10). For longer times the *100 CP* material is capable to form sufficiently dense and stable secondary plateaus, thanks to a sufficient amount of copper in the starting material and, thereby, in the secondary plateaus. From EDXS spectra (Fig. 14) referring to the secondary plateaus on *50 CP* and *100 CP* after 5h PoD tests, the concentration of

17

copper is 8 wt.% for the *100 CP* secondary plateaus, versus 2 wt.% only for *50 CP*. The higher availability of copper can stabilize the wear debris coming from the friction material, that indeed becomes the main component of the friction layer forming on the *100 CP* sample. This is not so for the *50 CP* material, whose secondary plateaus still display the irregular microstructure of the short term tests and are mostly made of iron oxide debris from the disc. This picture is coherent with the data for the specific wear coefficient in Table 4 and with the relevant plot in Fig. 9.
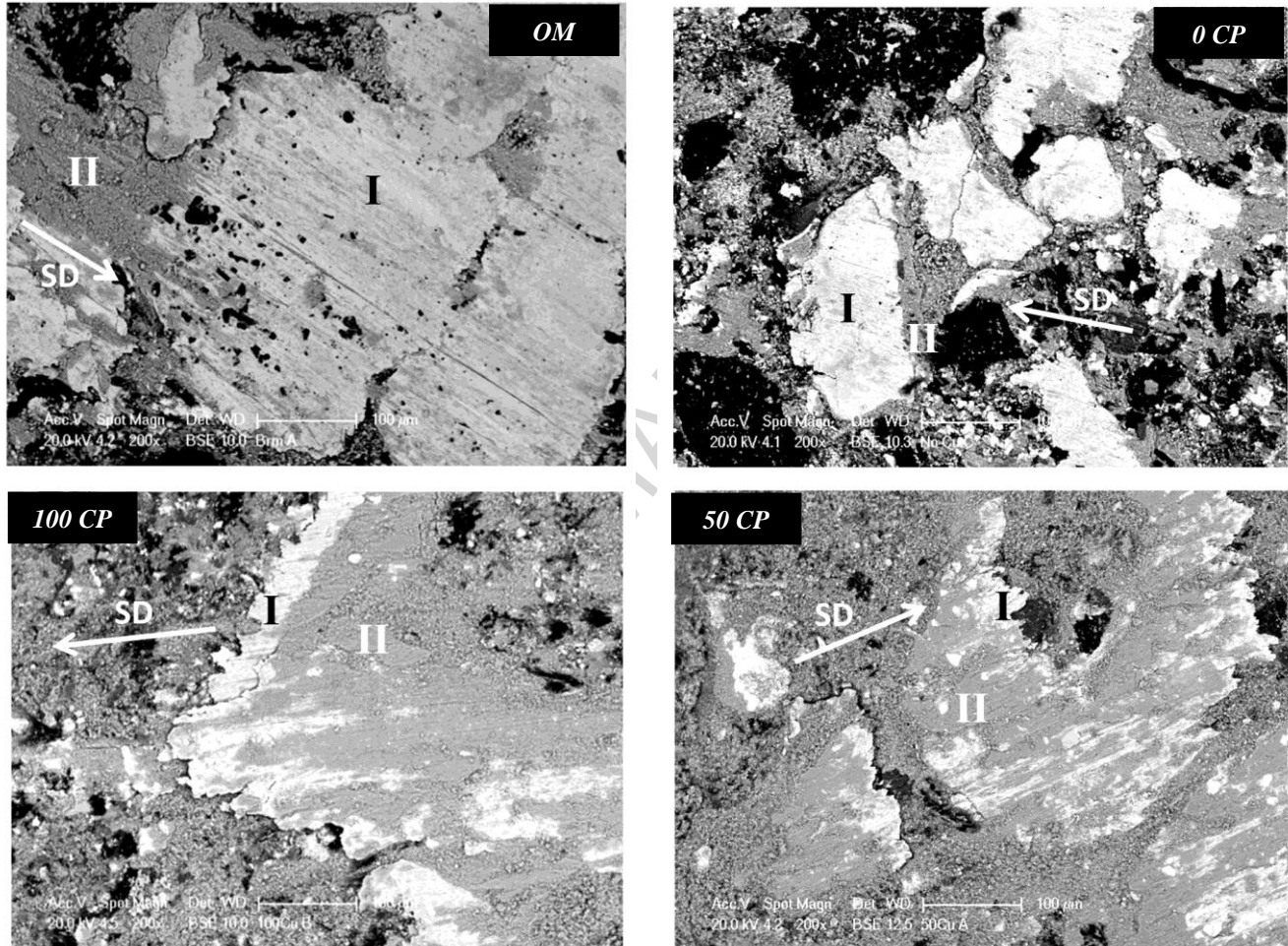
Fig.10: A comparison among plateaus observed on the pin surface after the short term (50 min) PoD tests. Legend: SD= sliding direction during pin-on-disc tests; I= primary plateau; II= secondary plateau.
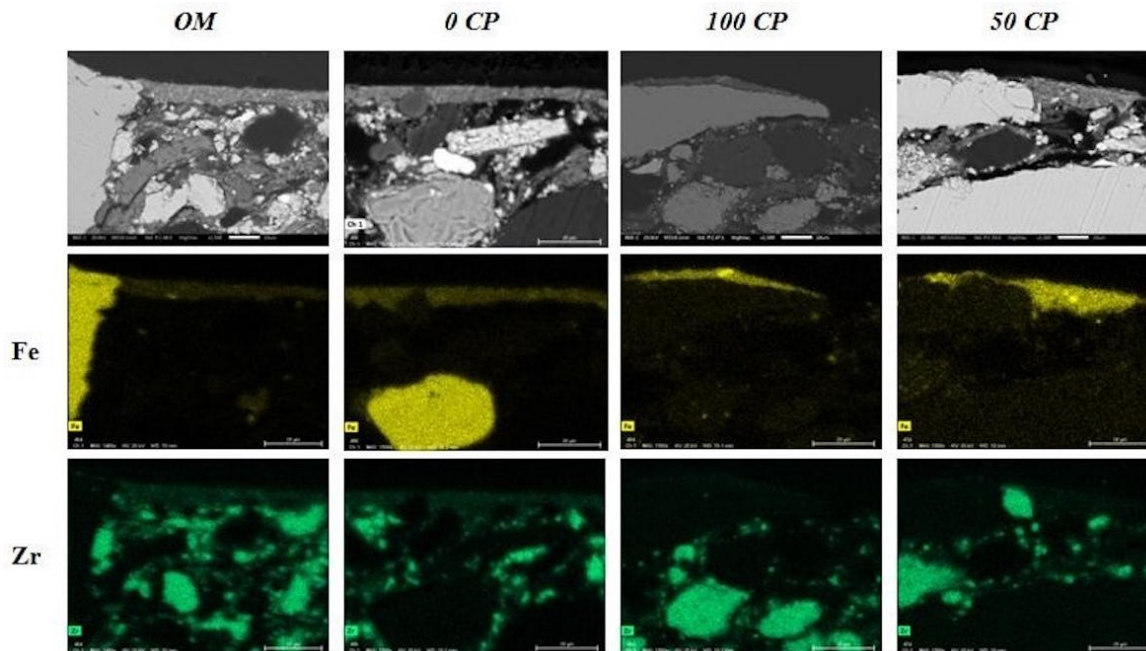
Fig.11: Cross-sectional SEM micrographs of the the surface regions of the pins made of the four friction materials: *OM, 0 CP, 100 CP* and *50 CP* after 50 min PoD tests. Relevant Fe and Zr X-Ray compositional maps show the spaitial distribution of these two elements.
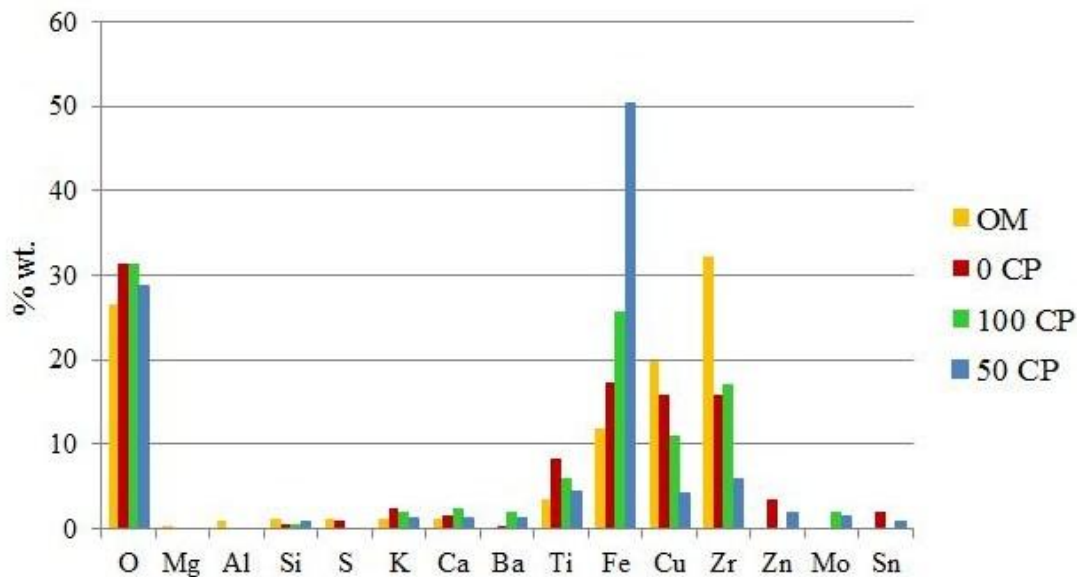

Fig.12 Diagram of the composition of the secondary plateaus that form during PoD on the pin surface after 50 min of sliding for the different friction materials considered: *OM, 0 CP, 50 CP* and *100 CP*.
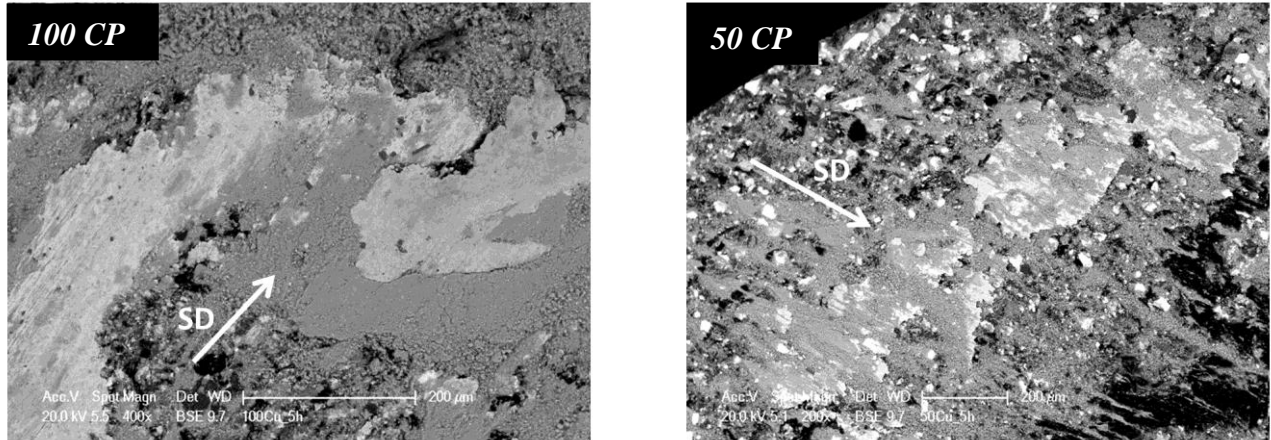
Fig.13 SEM micrographs of the top surface of the friction layer that formed on the *100 CP* and *50 CP* materials after the long term (5 h) PoD tests. SD: sliding direction during pin-on-disc tests.
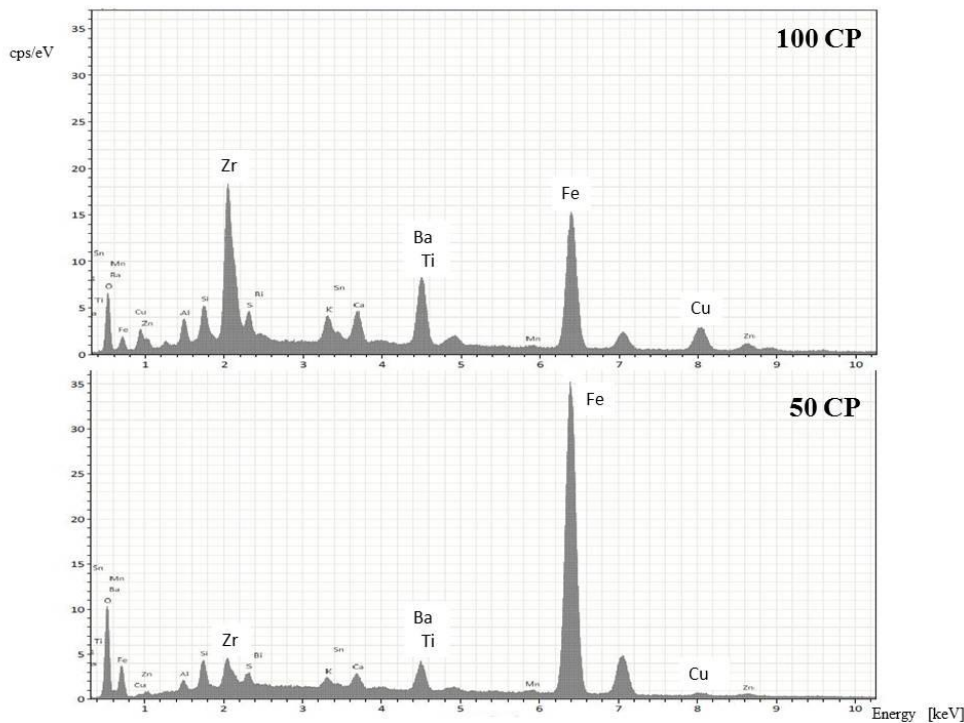

Fig. 14 Comparison between typical EDXS spectra acquired on the secondary plateaus of the *100 CP* (gray spectrum) and *50 CP* (red spectrum), respectively, after the long term (5h) PoD tests.

4. CONCLUSIONS and FUTURE PERSPECTIVES

The present investigation has confirmed the importance of copper in the formation of the friction layer, ensuring effective tribological performances of disc brake materials, wear tested using a PoD apparatus.

The main results obtained so far can be summarized as follows:

- The microstructural refinement of the copper powder, through high-energy ball-millling, has not achieved the expected results for a sort of *sequestration effect* of copper itself by the zirconia powder used as process control agent during ball-milling together with graphite.
- During ball-milling of the copper-zirconia-graphite mixture, copper promotes the clustering of the powder grains to form comparatively coarse composite copper-zirconia-graphite particles. This introduces inhomogeneities in the pins prepared for the tribological tests.
- Indeed, the formation of comparatively coarse composite copper-zirconia clusters has prevented both components from effectively entering the secondary plateaus of the friction layer.
- The pins made out of the *100 CP* powder sample require on average longer times to form a stable friction layer during the PoD tests, as compared to the reference *OM* material.
- Wear debris that remained trapped in between the mating surfaces partially spread over the metallic fibres present in the *50 CP* and 100 *CP* friction materials, thus reducing drastically their abrasion and consequent production of metallic fragments.
- These fragments, with particular regard for those coming from copper fibres, have a beneficial effect on the stabilization of the secondary plateaus, as proved by the behavior of the *0 CP* material.
- In this material, notwithstanding the lack of Cu powder, the friction layer has been stabilized by the copper particles produced by abrasive wear of the fibres exactly at the pin-disc interface, with the consequently high probability of being trapped into the friction layer.

The results presented herewith provide guidelines for perspective developments of the research. In particular:

- On the base of a comparison between the data obtained on the present research on *OM* material and the results presented in a previous paper [32], in which pins of *OM* cut from real brake pad were used, it can be stated that the powder metallurgy route for the direct forming of net-shape pins can be profitably used to explore minor changes in the formulations of the master friction materials, without the need of preparing large amount of master batches.
- The elimination of copper from friction materials may be pursued through its replacement with powders containing suitable components, that may be embedded and promote the formation of a stable friction layer.
- This may be achieved also through the controlled formation of wear debris from metallic fibres, mostly introduced as primary plateau formers.
- Since one of the main reasons for copper in the brake friction materials regards its beneficial effects on the high temperature performances, high temperatures PoD tests will be carried out since they may provide further interesting indications.
- In order to reduce the clustering effect that impairs the performance of the present samples, two ways, possibly to be jointly adopted, are suggested:
  - To carry out milling under moderately oxidizing atmosphere to promote the growth of an oxide surface layer on copper particles. This should reduce the bonding effect of Cu on ZrO_2 particles, coherently with the results obtained in a high energy ball milling study on Cu [44].
 - To increase the percentage of graphite in the mix.

21

5.REFERENCES

[1] J. Wahlström, L. Olander, U. Olofsson, Size, Shape, and Elemental Composition of Airborne Wear Particles from Disc Brake Materials, Tribol Lett 38 (2010) 15–24.

[2] T. Grigoratos, G. Martini, Non-exhaust Traffic Related Emissions. Brake and Tyre Wear PM. Literature Review, Report EUR 26648 EN. European Union (2014) Luxembourg.

[3] UN GRPE-PMP informal Group/JRC, Particle emissions from Tyre and brake wear on-going literature review (2014).

[4] M. Kchaou, A. Sellami, R. Elleuch, H. Singh, Friction characteristics of a brake friction material under different braking conditions, Mater. and Des. 52 (2013) 533-540.

[5] K.W. Liew, U. Nirmal, Frictional performance evaluation of newly designed brake pad materials, Mater. and Des. 48 (2013) 25–33.

[6] F. Eddoumy, H. Kasem, H. Dhieb, J.G. Buijnsters, P. Dufrenoy, J.P. Celis, Y.Desplanques, Role of constituents of friction materials on their sliding behavior between room temperature and 400 °C, Mater. and Des. 65 (2015) 179-186.

[7] A. Sellami, M. Kchaou, R. Elleuch, A.L. Cristol, Y. Desplanques, Study of the interaction between microstructure, mechanical and tribo-performance of a commercial brake lining material, Mater. and Des. 59 (2014) 84–93.

[8] D. Chan, G.W. Stachowiak, Review of automotive brake friction materials, J.Automobile Engineering, Proc.Instn.Mech.Engrs Vol.218 Part D (2004) 953-966.

[9] J. Bijwe, Composites as friction materials: recent developments in non-asbestos fiber reinforced friction materials – a review, Polym.Compos.18 (1997) 378–396.

[10] G. Straffelini, Friction and Wear, Methodologies for Design and Control, Springer, The Netherlands, 2015.

[11] P. Filip, Z. Weiss, D. Rafaja, On friction layer formation in polymer matrix composite materials for brake applications,Wear 252 (2002) 189–198.

[12] M. Eriksson, S. Jacobson, Tribological surfaces of organic brake pads, Tribology International 33 (2000) 817–827.

[13] W. Österle, I. Dörfel, C. Prietzel, H. Rooch, A.L. Cristol–Bulthé, G. Degallaix, Y. Desplanques, A comprehensive microscopic study of third body formation at the interface between a brake pad and brake disc during the final stage of a pin–on–disc test, Wear 267 (2009) 781–788.

[14] California State Senate Bill 346: "Hazardous materials: motor vehicle brake friction materials",

http://www.leginfo.ca.gov/pub/09-10/bill/sen/sb_0301- 0350/sb_346_bill_20100927_chaptered.pdf.

[15] Washington State Senate Bill 6557: "Brake Friction Material - Restriction on Use",
http://apps.leg.wa.gov/documents/billdocs/2009-10/Pdf/Bills/Session%20Law%202010/6557-
S.SL.pdf.

[16] J. Kukutschová, V. Roubíček, K. Malachová, Z. Pavlíčková, R. Holuša, J. Kubačková, V. Mička, D. MacCrimmon, P. Filip, Wear mechanism in automotive brake materials, wear debris and its potential environmental impact, Wear 267 (2009) 807–817.

[17] R. Franco, R. Sánchez-Olea, E.M. Reyes-Reyes, M.I. Panayiotidis, Environmental toxicity, oxidative stress and apoptosis: Ménage à Trois, Mutation Research 674 (2009) 3–22.

[18] F. Solomon, Impacts of copper on aquatic Ecosystems and human health, MINING.com (2009) 25-28.

[19] W. Österle, C. Deutsch, T. Gradt, G. Orts-Gil, T. Schneider, A.I. Dmitriev, Tribological screening tests for the selection of raw materials for automotive brake pad formulations, Tribology International 73 (2014) 148–155.

[20] B.D. Garg, S.H. Cadle, P.A. Mulawa, P.J. Groblicki, Brake wear particulate matter emissions, Environ. Sci. Technol. 34 (2000) 4463–4469.

[21] P.G. Sanders, N. Xu, T.M. Dalka, M. Maricq, Airborne brake wear debris: size distributions, composition, and a comparison of dynamometer and vehicle tests, Environ. Sci. Technol. 37 (2003) 4060–4069.

[22] Brake Pad Partnership, Characterization of Airborne Brake Wear Debris, Final Report, 2006. http://www.suscon.org/brakepad/pdfs/ADPSDAmendedFinalReport(Jan2006).pdf.

[23] A.K. Lund., J. Lucero, S. Lucas, M.C. Madden, J.D. McDonald, J.C. Seagrave, T.L. Knuckles, M.J. Campen, Vehicular emissions induce vascular MMP-9expression and activity associated with endothelin-1-mediated pathways, Arterioscler. Thromb. Vasc. Biol. 29 (2009) 511-517.

[24] J.A. Araujo, A.E. Nel, Particulate matter and atherosclerosis: role of particle size, composition and oxidative stress, Part. And Fibre Toxicol. (2009) 6-24.

[25] Y.C. Huang, A.J. Ghio, J. Stonehuerner, J. McGee, J.D. Carter, S.C. Grambow, R.B. Devlin, The role of soluble components in ambient fine particles-induced changes in human lungs and blood, Inhal. Toxicol. 15 (2003) 327-342.

[26] R.A. Peters, Environmental Effects of Copper in Brake Pad Wear Debris, Brake Pad Partnership, Brake Colloquium & Exhibition, Oct.12–15(2008). San Antonio, Texas, USA.

[27] W. Österle, C. Prietzel, H. Kloß, A.I. Dmitriev, On the role of copper in brake friction materials, Tribology International 43 (2010) 2317-2326.

[28] W. Österle, M. Griepentrog, T. Gross, I. Urban, Chemical and microstructural changes induced by friction and wear of brakes, Wear 251 (2001) 1469–1476.

[29] M. Eriksson, F. Bergman, S. Jacobson, On the nature of tribological contact in automotive brakes, Wear 252 (2002) 26–36.

[30] M. Kumar, J. Bijwe, Non-asbestos organic friction composites: Role of copper; its shape and amount, Wear 270 (2011) 269-280.

[31] G. Straffelini, R. Ciudin, A. Ciotti, S. Gialanella, Present knowledge and perspectives on the role of copper in brake materials and related environmental issues: A critical assessment, Environmental Pollution, 207 (2015) 211-219.

[32] P.C. Verma, L. Menapace, A. Bonfanti, R. Ciudin, S. Gialanella, G. Straffelini, Braking pad-disc system: Wear mechanisms and formation of wear fragments, Wear 322-323 (2015) 251-258.

[33] P.C. Verma, R. Ciudin, A. Bonfanti, P. Aswath, G. Straffelini, S. Gialanella, Role of the friction layer in the high-temperature pin-on-disc study of a brake material, Wear 346-347 (2016) 56-65.

[34] P.C. Verma, I. Metinoz, R. Ciudin, G. Perricone, G. Straffelini, S. Gialanella, Wear behavior of a low metallic friction material dry sliding against a cast iron disc: Role of the heat-treatment of the disc, Wear, 348-349 (2016) 10-16.

[35] W. Österle, A.I. Dmitriev, Functionality of conventional brake friction materials – Perceptions from findings observed at different length scales, Wear 271 (2011) 2198-2207.

[36] M. Kumar, J. Bijwe, Role of different metallic fillers in non-asbestos organic (NAO) friction composites for controlling sensitivity of coefficient of coefficient of friction to load and speed, Tribology International 43 (2010) 965-974.

[37] H. Jang, K. Ko, S.J. Kim, R.H. Basch, J.W. Fash, The effect of metal fibers on the friction performance of automotive brake friction materials, Wear 256 (2004) 406-414.

[38] S. Gialanella, L. Lutterotti, Nanocrystalline metallic materials, Nanoclusters and Nanocrystals, H.S. Nalwa ed., American Scientific Publisher (2003) 1-52.

[39] M. Aliofkhazraei ed., Handbook of Mechanical Nanostructuring, 2 vol., M. Aliofkhazraei ed., John Wiley & Sons, 2015.

[40] I.M. Hutchings, Friction and Wear of Engineering Materials, Edward Arnold, London, 1992.

[41] M. Zakeri, M. Razavi, M.R. Rahimipour, B. JamalAbbasi, Effect of ball to powder ratio on the ZrO_2 phase transformations during milling, Physica B 444 (2014) 49-53.

[42] S. Bid, S.K. Pradhan, Preparation and microstructure characterization of ball-milled ZrO_2 powder by the Rietveld method: monoclinic to cubic phase transformation without any additive, J.Appl.Cryst. 35 (2002) 517-525.

[43] G. Straffelini, L. Maines, The relationship between wear of semimetallic friction mterials and pearlitic cast iron in dry sliding, Wear 307 (2013) 75-80.

[44] C. Menapace, G. Cipolloni, M. Hebda, G. Ischia, Spark plasma sintering behaviour of copper powders having different particle sizes and oxygen contents, Powder Technology 291 (2016) 170-177.
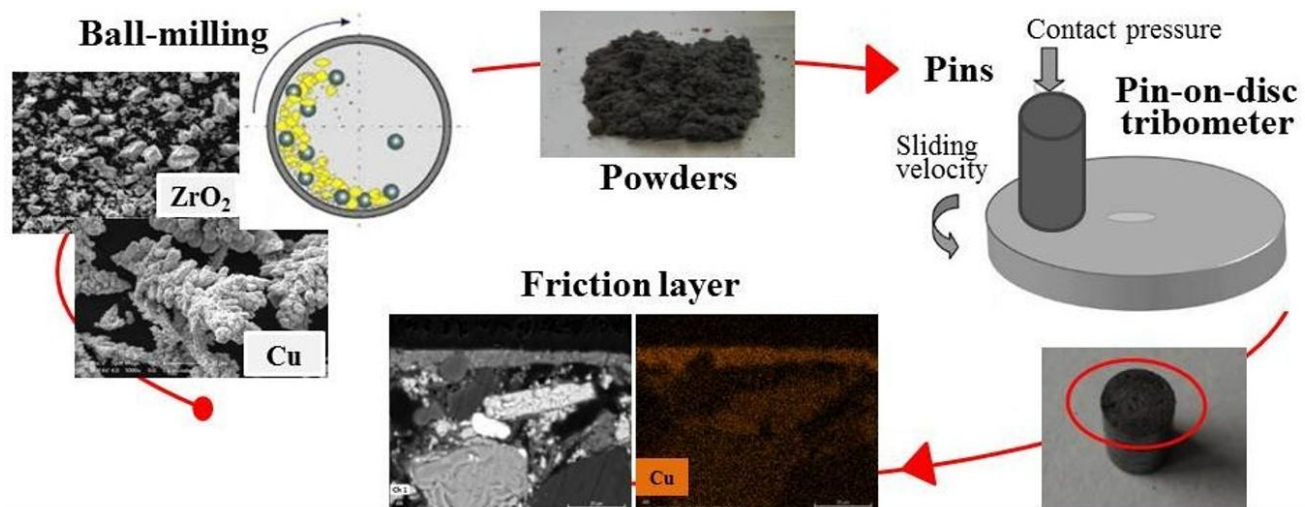
Graphical abstract

Highlights

- The role of the copper has been studied with the aim of reducing its concentration in brake friction materials.
- The design of the friction material was changed introducing two of the initial composition ingredients, nanostructured after ball-milling.
- Ball milling induced the formation of Cu-ZrO_2 clusters that influence the tribological behavior of the new formulation materials.
- Even in the absence of copper particles, a good friction layer is formed thanks to the wearing of copper fibers.